Proof Delivery Form

Journal and Article number: BCJ-2020-0360

Number of pages (not including this page): 15

Biochemical Journal

Please check your proof carefully to ensure (a) accuracy of the content and (b) that no errors have been introduced during the production process.

- You are responsible for ensuring that any errors contained in this proof are marked for correction before publication. Errors not marked may appear in the published paper.
- Corrections should only be for typographical errors in the text or errors in the artwork; substantial revision of the substance of the text is not permitted.
- Please answer any queries listed below.
- If corrections are required to a figure, please supply a new copy.

Your proof corrections and query answers should be returned as soon as possible (ideally within 48 hours of receipt). Please upload your corrected proof and any additional files (e.g. artwork) via the online proof review page from which you downloaded this file. You can also provide any specific instructions or comments in the 'Response Comments' box on the online page.

Notes:

1. Please provide the paper's reference number in any correspondence about your article
2. If you have any queries, please contact the publisher by email (production@portlandpress.com) or by telephone +44 (0)20 7685 2410

Supplementary Material:

This proof does not contain any supplementary material. If supplementary content is associated with this article it will be published, in the format supplied by the authors, with the online version of the article.

Queries for author:

Q1: Please review the highlighting of the author surnames. Bearing in mind that this will direct how the authors are indexed by the journal and PubMed, please confirm if this is correct or indicate any changes that are needed.

Q2: Please confirm that this statement is an accurate reflection of any competing interests (or lack thereof) of the author(s).

Q3: Please confirm that all sources of funding (including all relevant grant numbers) have been acknowledged in Funding section.

Biochemical Journal (2020) **0** 1–15
https://doi.org/10.1042/BCJ20200360

PORTLAND PRESS

Research Article

Role of sialidase Neu3 and ganglioside GM3 in cardiac fibroblasts activation

Andrea Ghiroldi[1,*], Marco Piccoli[1,*], Pasquale Creo[1], Federica Cirillo[1], Paola Rota[2], Sara D'Imperio[1,3,4], Giuseppe Ciconte[4], Michelle M. Monasky[4], Emanuele Micaglio[4], Andrea Garatti[5], Massimo Aureli[6], Emma Veronica Carsana[6], Lorenzo Menicanti[5], Carlo Pappone[4,7] and Luigi Anastasia[1,7]

[1]Laboratory of Stem Cells for Tissue Engineering, IRCCS Policlinico San Donato, San Donato Milanese, Milan, Italy; [2]Department of Biomedical, Surgical and Dental Sciences, University of Milan, Milan, Italy; [3]Department of Biomedical Sciences for Health, University of Milan, Milan, Italy; [4]Arrhythmology Department, IRCCS Policlinico San Donato, San Donato Milanese, Milan, Italy; [5]Department of Cardiovascular Disease 'E. Malan', Cardiac Surgery Unit, IRCCS Policlinico San Donato, San Donato Milanese, Milan, Italy; [6]Department of Medical Biotechnology and Translational Medicine, University of Milan, Milan, Italy; [7]University of Vita-Salute San Raffaele, Milan, Italy

Correspondence: Luigi Anastasia (anastasia.luigi@hsr.it)

Cardiac fibrosis is a key physiological response to cardiac tissue injury to protect the heart from wall rupture. However, its progression increases heart stiffness, eventually causing a decrease in heart contractility. Unfortunately, to date, no efficient antifibrotic therapies are available to the clinic. This is primarily due to the complexity of the process, which involves several cell types and signaling pathways. For instance, the transforming growth factor beta (TGF-β) signaling pathway has been recognized to be vital for myofibroblasts activation and fibrosis progression. In this context, complex sphingolipids, such as ganglioside GM3, have been shown to be directly involved in TGF-β receptor 1 (TGF-R1) activation. In this work, we report that an induced up-regulation of sialidase Neu3, a glycohydrolytic enzyme involved in ganglioside cell homeostasis, can significantly reduce cardiac fibrosis in primary cultures of human cardiac fibroblasts by inhibiting the TGF-β signaling pathway, ultimately decreasing collagen I deposition. These results support the notion that modulating ganglioside GM3 cell content could represent a novel therapeutic approach for cardiac fibrosis, warranting for further investigations.

Introduction

Fibrosis is a physiological process common to many organs, such as kidney [1], liver [2], lungs [3], and heart [4–6], which is characterized by the deposition of extracellular matrix (ECM) proteins in response to an injury [7]. Therefore, fibrosis is considered primarily as a reparative mechanism, since it promotes tissue healing. However, when not properly controlled, it could become pathologic, leading to parenchymal scarring, tissue remodeling and, eventually, to organ failure [8]. In this context, cardiac fibrosis has been defined as either reactive fibrosis or replacement fibrosis, depending on the stimuli [8]. Replacement fibrosis occurs after a massive loss of cardiomyocytes, as for example after myocardial infarction. Given the low regenerative capacity of the heart [9], the repair process aims to replace the dead cardiomyocytes with a fibrotic scar produced by activated fibroblasts. This response is fundamental, since it stabilizes ventricular walls, ultimately preventing their rupture [10]. However, its uncontrolled progression provokes chamber dilatation and hypertrophy, increases stiffness, and impairs electrical coupling, ultimately leading to heart failure [11]. Cardiac fibroblasts are the principal players of this mechanism and, upon appropriate stimuli, they can transdifferentiate into their active form, i.e. cardiac myofibroblasts [4]. Interestingly, cardiac fibroblasts are a peculiar cell type of embryonic epicardial and endothelial origins [12]. Their primary role is to furnish structural support for cardiomyocytes, regulating the homeostasis of the ECM [13]. Furthermore, they distribute mechanical forces and mediate electrical conduction [14]. After tissue injury, cardiomyocytes become apoptotic, endothelial cells modulate the inflammatory response, and proliferating immune cells

*These authors contributed equally to this work.

Received: 5 May 2020
Revised: 13 August 2020
Accepted: 1 September 2020

Accepted Manuscript online: 1 September 2020
Version of Record published: 0 Month 2020

Biochemical Journal (2020) **0** 1–15
https://doi.org/10.1042/BCJ20200360

infiltrate the damaged myocardium [15], causing an increase in inflammation and in profibrotic cytokines that activate cardiac fibroblasts. Differentiation towards myofibroblasts is characterized by the production of ECM proteins, such as collagen and fibronectin, and by the expression of stress fibers, composed mostly by α-smooth muscle actin (α-SMA), which is involved in the contractile activity [16]. The master regulator of fibrosis induction is TGF-β [17]: this cytokine binds to a heterodimeric membrane receptor composed of two subunits (TGF-β R1 and TGF-β R2), activating its intracellular canonical signaling cascade, including Smad family members [18]. The binding of TGF-β to its receptor induces the phosphorylation of the receptor-regulated members of the Smad family (R-Smads), Smad2 and Smad3, which, in turn, interact with Smad4 and translocate as a complex to the nucleus, activating profibrotic gene expression [17]. TGF-β signaling is finely regulated, and the receptors represent the first step for its modulation [19]. Different factors could influence the activity of TGF-β receptors, such as proteins involved in ubiquitination [20], other receptors (i.e. endoglin [21] or ALK2/3/6 [22]), proteins involved in their trafficking towards the membranes (i.e. Rab GTPases [23], caveolin-1 [24]), or molecules that increase TGF-β response (i.e. ganglioside GM3 [25]). Among these factors, it has been demonstrated that ganglioside GM3 boosts the effects of TGF-β through the direct interaction with the TGF-β R1 in human lens epithelial cells, promoting the epithelial-to-mesenchymal transition [25]. Ganglioside GM3 is a member of the ganglioside family, which are glycosphingolipids containing sialic acid implicated in various biological processes, such as cell proliferation, cell interaction, differentiation, signal transduction, and stem cell markers [26–28]. GM3 could alter the activity of the membrane receptors of insulin, VEGF, EGF, or FGF; thus, it is implicated in different pathological processes, like obesity, insulin resistance, and tumor progression [29]. Its levels are tightly regulated by its synthesis by GM3 synthase [30], and by its degradation by Neu3 sialidase [31,32]. Sialidase Neu3 is a membrane glycosidase that removes sialic acid from GD1a and GM3 gangliosides [33] and is implicated in different cellular functions, including cell proliferation and differentiation [31,34]. We previously demonstrated that Neu3 is activated under hypoxic conditions both *in vitro* [35] and *in vivo* [36] and that its effects are mainly exerted by modulation of GM3 levels [31,33,35].

In this work, we assessed the effects of Neu3 overexpression on cardiac fibroblasts activation in a cellular model of cardiac fibrosis in order to identify new possible pharmacological targets for the development of new drugs for cardiac fibrosis modulation.

Materials and methods

Ethical statement

All subjects gave their informed consent for inclusion before they participated in the study. The study was conducted in accordance with the Declaration of Helsinki, and the protocol was approved by the Ethics Committee of the ASL MilanoDue (Protocol n. 2385).

Cardiac fibroblast isolation, culture, and stable overexpression of NEU3

Right atrial appendage biopsies were obtained from the point of atrial cannulation at the beginning of extracorporeal circulation. Tissue specimens weighed ∼100 mg and were collected in cold phosphate buffer solution (PBS) at pH 7.4, kept in ice, and processed within minutes after collection. Samples were washed with phosphate-buffered saline, cut into small pieces, and placed in the cell culture dish pre-coated with 1% porcine skin gelatin with 2 ml of growth medium composed of DMEM (Merck), with low glucose concentration (1 g/L), supplemented with 10% (v/v) fetal bovine serum (FBS) (Merck), 2 mM glutamine (Merck), and penicillin/streptomycin 1X (Euroclone). Once the pieces attached to the plate, the growth medium was added up to 7 ml. The fibroblasts started to grow from the minced fragments in 2–3 days. When there were sufficient cells, they were detached enzymatically and plated in new dishes for proliferation. Cardiac fibroblasts stably overexpressing NEU3 sialidase were prepared with a lentiviral vector, according to our previously developed methods [37].

Flow cytometry

Isolated cells were characterized by flow cytometry for the expression of fibroblasts markers and to test the level of contamination with other cell types. Briefly, cells were stained with a three-step procedure: (1) incubation for 30 min at 4°C with 50% FBS (Merck) in PBS to block the Fc receptor, (2) incubation with conjugated mouse antihuman antibodies at the optimal concentration (1 : 20 dilution) in PBS for 10 min at 4°C, and (3) two washes with PBS at 4°C. Samples were analyzed with a Navios cytofluorimeter (Beckman Coulter), and data were processed with Kaluza software (Beckman Coulter). Cell characterization was performed using the

following antibodies: CD9-FITC, CD29-PE, CD34-PERCP-eFluor 710, CD44-FITC, CD45-PE, CD73-FITC, CD90-PE, CD105-PE, CD106-PE, CD117-FITC, CD146-PE, and HLA-DR-FITC.

Fibroblasts activation

Cardiac fibroblasts were plated at 80–90% confluency and serum-starved for 48 h. Then, human recombinant TGF-β isoform 1 (Peprotech) was added to a final concentration of 10 ng/ml for 72 h.

Immunofluorescence

Cardiac fibroblasts were rinsed twice with PBS and then fixed using a solution of 4% paraformaldehyde in PBS for 15 min at room temperature. Fixed cells were washed with PBS three times for 5 min. Samples were then treated with blocking solution (PBS, 5% goat serum, Tween-20 0.1%) for 1 h at RT. Cells were then incubated with the primary antibody mouse monoclonal anti-α-Smooth muscle actin (α-SMA) (1 : 200, #A52228, Merck) for 2 h at RT. Cells were then washed with PBS, three times for 5 min, and incubated with secondary antibody (FITC goat anti-mouse, Jackson Laboratories; dilution 1 : 500 in blocking solution), 1 h at RT. Samples were finally washed with PBS (three times for 5 min) and incubated for 15 min with 4′,6′ diamino-2-phenylindole (DAPI) solution (Merck, Italy; dilution 1 : 2500 in deionized water). After being washed twice, images were acquired with a fluorescence microscope (Leica DM IRBE, Leica Microsystems Srl, Italy).

RNA extraction and Real Time PCR

Total RNA was isolated using the ReliaPrep™ RNA Miniprep System (Promega), following the manufacturer's instructions. Then, 1 μg of RNA was reverse transcribed to cDNA with the iScript cDNA synthesis kit (Bio-Rad), according to the manufacturer's instructions. Real time PCR was performed with 10 ng of cDNA template, 0.2 μm primers, and 1× GoTaq® qPCR Master Mix (Promega) in 20 μl of final volume, using a StepOnePlus® real time PCR system (Applied Biosystem). The amplification protocol was: 95°C for 2 min, 40 cycles of 5 s each at 95°C, 30 s at 57°C and 30 s at 72°C, and a final stage at 72°C for 2 min. Relative quantification of target genes was calculated by the equation $2^{-\Delta\Delta Ct}$ using two housekeeper genes (S14 and UBC). The primer sequences are reported in Table 1.

Western blot

For protein expression analysis, cardiac fibroblasts were lysed with RIPA buffer (1% Nonidet P-40 in 50 mm Tris–HCl, pH 7.5, 150 mm NaCl, 0.1% sodium deoxycholate, 1% protease inhibitor cocktails), incubated in ice for 30 min, and then centrifuged at 13 000×***g*** for 15 min at 4°C. The supernatant was collected, and the total amount of proteins was determined with BCA assay (Pierce), following the manufacturer's instructions. Proteins (20 μg) were resolved on a 10% SDS–PAGE gel and subsequently transferred onto nitrocellulose membranes by electroblotting. The total amount of transferred proteins, used for the normalization of detected proteins, was determined with the REVERT Total Protein Stain kit (LI-COR Biotechnology), following manufacturer's instructions. Membranes were incubated with blocking buffer (TBS: 10 mm Tris–HCl, pH 7.4, 150 mm NaCl, 0.1% (v/v) Tween 20 containing 5% (w/v) dried milk or 5% (w/v) bovine serum albumin) for 1 h at RT, and then the primary antibodies were added and incubated overnight at 4°C in the proper blocking

Table 1 Primer used for Real Time PCR

Gene	Forward primer	Reverse primer
ACTA2	5′-CTGGACTCTGGAGATGGTG-3′	5′-GCAGTAGTAACGAAGGAATAGC-3′
Collagen I	5′-CGACCTGGTGAGAGAGGAGTTG-3′	5′-AATCCATCCAGACCATTGTGTCC-3′
Neu3	5′-TGGTCATCCCTGCGTATACC-3′	5′-TCACCTCTGCCACTTCACAT-3′
GM3 synthase	5′-CTGCCTTTGACATCCTTCAGT-3′	5′-CGATTGTGGGGACGTTCTTA-3′
Sp1	5′-ATCATCACAAGCCAGTTCCA-3′	5′-AGATGTCTGGTTTGCTGGA-3′
Sp3	5′-AGTGGGCAGTATGTTCTTCC-3′	5′-TTTGAACCTGCTGACCATCT-3′
UBC	5′-CTGGAAGATGGTCGTACCCTG-3′	5′-GGTCTTGCCAGTGAGTGTCT-3′
S14	5’-GTGTGACTGGTGGGATGAAGG-3′	5′-TTGATGTGTAGGGCGGTGATAC-3′

Biochemical Journal (2020) **0** 1–15
https://doi.org/10.1042/BCJ20200360

solution. The following primary antibodies were used: anti-α-SMA (1 : 5000, #A52228, Merck), anti-collagen I (1 : 1000, #PA1-26204, Invitrogen), anti-TGF-β Receptor I (1 : 1000, # AH01552, Thermo Fisher), anti-phospho-TGF-β Receptor I Ser-165 (1 : 1000, #PA5-40298, Thermo Fisher), anti-SMAD2 (1 : 1000, #436500, Thermo Fisher), anti-phospho-SMAD2 Ser465/Ser467 (1 : 1000, #44-244G, Thermo Fisher), anti-SMAD7 (1 : 1000, #42-0400, Thermo Fisher), and anti-GM3 synthase (1 : 1000, #sc365329, Santa Cruz). The membranes were washed three times with TBS-Tween 20 for 10 min and then incubated for 2 h with the appropriate secondary antibody. The secondary antibodies used were: anti-mouse HRP conjugated (Amersham), anti-rabbit HRP conjugated (Amersham), IRDye 800CW anti-mouse (Licor), IRDye 800CW anti-rabbit (Licor), IRDye 680CW anti-mouse (Licor), and IRDye 680CW anti-rabbit (Licor). After three washes with TBS-Tween 20, proteins were detected with an ECL detection kit (Cyanagen) or with infrared acquisition at the proper wavelength with the LI-COR Odyssey Infrared Imaging System (LI-COR Biotechnology).

Sialidase activity assay

Cells were collected by scraping and resuspended in PBS containing protease inhibitor and phosphatase inhibitor cocktails (Merck). Pulse sonication was used to lyse cells (10 pulses of 0.5 s in ice). The lysate was centrifuged at 800×***g*** for 10 min at 4°C, and the membrane fraction was then separated by centrifugation at 200 000×***g*** for 20 min at 4°C with a TLC100 Ultracentrifuge (Beckman Coulter). Total protein content was determined with the BCA protein assay kit (Pierce), following the manufacturer's instructions. The sialidase activity present in the membrane fractions was assayed using 4-MU-NeuAc at pH 3.8 according to a well-established protocol [35]. One milliunit of sialidase activity is defined as the amount of enzyme liberating 1 nmol of product (4-MU) per min.

Treatment of cell cultures with [3-^{3}H]sphingosine

The determination of the GM3 content in scramble, Neu3 overexpressing and shGM3 cells was performed by radioactive metabolic labeling, as previously described [38]. [3-^{3}H]sphingosine (PerkinElmer Life Sciences) was dissolved in methanol, transferred into a sterile glass tube, and then dried under a nitrogen stream. The residue was dissolved in growth medium to obtain a final sphingosine concentration of 30 nM (corresponding to 0.4 μCi/100 mm dish). An amount of 1×10^6 cells were incubated in this medium for a 2 h pulse followed by a 24 h chase, a condition warranting a steady-state metabolic condition. At the end of the 24 h chase, cells were harvested and lyophilized.

Lipid extraction and analyses

Total lipids from lyophilized cells were extracted twice with chloroform/methanol 2 : 1 (v/v) and with chloroform/methanol/water 20 : 10 : 1 (v/v/v), respectively. The resulting lipid extracts were dried under a nitrogen stream and dissolved in chloroform/methanol 2 : 1 (v/v) at room temperature. Lipid extracts were analyzed by HPTLC carried out with the solvent system chloroform/methanol/0.2% aqueous $CaCl_2$, 50 : 42 : 11 (v/v/v). The total lipid extracts were subjected to partitioning in chloroform/methanol/water, 2 : 1 (v/v) and 20% water. The aqueous phase, containing gangliosides, was counted for radioactivity and subjected to HPTLC separation, loading the same amount of proteins in each lane, corresponding to at least 1400 dpm, using the solvent systems chloroform/methanol/0.2% aqueous $CaCl_2$, 60 : 40 : 9 (v/v). [3-^{3}H]Sphingolipids were identified by referring to radiolabeled standards and quantified by radiochromatoimaging (Beta-Imager 2000; Biospace).

Sirius Red staining

Sirius Red staining for the quantification of extracellular collagen deposition was performed according to Tullberg-Reinert et al. [39]. Briefly, cells were washed twice with PBS and then fixed for 1 h with Bouin's fluid (71% saturated picric acid, 24% formaldehyde, 5% glacial acetic acid). Cells were washed with tap water for 15 min and air-dried. Then, Sirius Red reagent (1 mg/ml in saturated picric acid, Merck) was added, and the cells were incubated under agitation for 1 h. After two washes with 0.01 N hydrochloric acid, the images were acquired with a microscope. The dye was then dissolved, incubating the cells with 0.2 ml of 0.1 N sodium hydroxide for 30 min under agitation. The dye solution was transferred to a 96-well plate and the optical density measured with a VarioskanLux multiplate reader at 550 nm.

GM3 silencing

Specific siRNA duplexes targeting GM3 synthase, siRNA transfection reagents, and reduced-serum transfection medium were purchased from Santa Cruz Biotechnology. The day before transfection, 7×10^5 cardiac fibroblasts were seeded in each well of a 12-well cell culture plate in DMEM low glucose, containing 10% FBS without antibiotics and incubated for 24 h at 37°C and 5% CO_2. The next day, transfection complexes were prepared using GM3 synthase siRNA, siRNA transfection reagent, and transfection medium, according to the

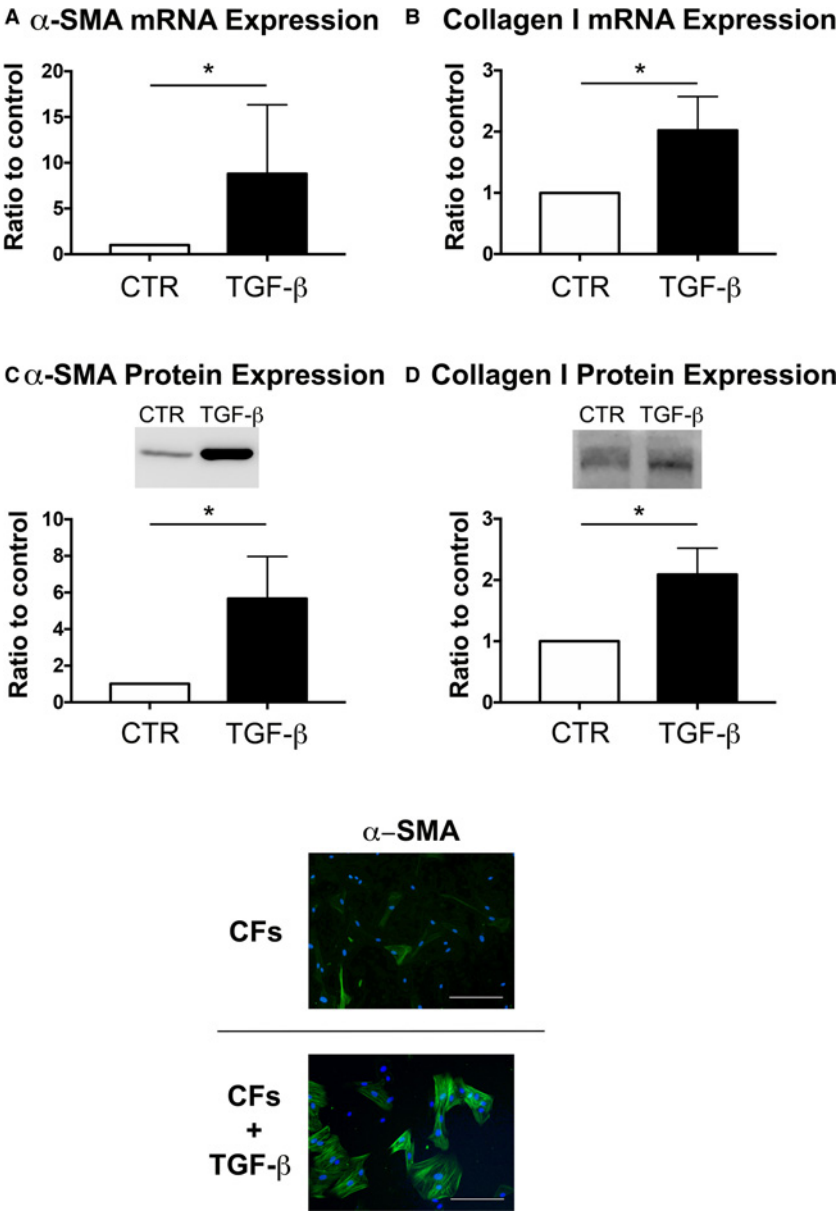

Figure 1. Fibrosis induction in cardiac fibroblasts after TGF-β treatment.

Cardiac fibroblasts were treated for 72 h with TGF-β (10 ng/ml) to induce fibrosis and the expression of fibrotic markers was analyzed. (**A** and **B**) mRNA expression of α-SMA and collagen I through RT-PCR. (**C** and **D**) Protein expression of α-SMA and collagen I through Western Blot analysis. (**E**) Immunofluorescence analysis of α-SMA expression (green) in TGF-β stimulated cells. Cell nuclei were stained with DAPI (blue). Data are presented as mean ± SD of four independent experiments. Results are expressed as fold change, in comparison with untreated cells. Scale bar 100 μm. Statistical significance was determined by Student's *t*-test. (*) $P < 0.05$.

Biochemical Journal (2020) **0** 1–15
https://doi.org/10.1042/BCJ20200360

manufacturer's protocol, and were added to each well. The final concentration of GM3 synthase siRNA duplexes used was 3 μg. A scrambled siRNA (Santa Cruz Biotechnology) was used as negative control.

Statistical analysis

The Student's *t*-test or the one-way ANOVA, followed by the Bonferroni's multiple comparison test, were used to determine significance using GraphPad Prism 7 software. *P* values of less than 0.05 were considered to be significant. All *P* values were calculated from data obtained from at least three independent experiments. All error bars represent the standard deviation of the mean.

Results

Fibroblasts activation upon TGF-β treatment

Isolated cardiac fibroblasts were phenotypically characterized by flow cytometry, analyzing the expression of the fibroblasts markers, of mesenchymal markers, and of immune system cells markers, to assess the purity of the isolated population. As expected, the cells were highly positive for CD9, CD29, CD44, CD73, CD90, and CD105 [40], and with low or null positivity for CD34, CD45, CD106, CD117, and HLA-DR (Supplementary Figure S1) [41]. Then, fibroblasts activation was induced with TGF-β. The treatment caused a marked increase in α-SMA and collagen I at both mRNA (Figure 1A,B) and protein levels (Figure 1C,D). Moreover, cells showed a morphological alteration, characterized by the formation of actin stress fibers, a hallmark of myofibroblasts differentiation (Figure 1E). Interestingly, TGF-β treatment induced an alteration in Neu3 genic expression and enzymatic activity. In particular, Neu3 mRNA expression and activity were significantly reduced by 25% (Figure 2A) and 50% (Figure 2B), respectively. Then, we analyzed the expression of Sp1 and Sp3, the two principal transcription factors that control Neu3 expression, and both resulted significantly reduced of 35% (Figure 2C) and 25% (Figure 2D), respectively.

Neu3 overexpression reduces fibroblasts activation

Cardiac fibroblasts were infected with a lentiviral vector containing the human Neu3 sialidase gene or with a lentiviral scramble vector. Then, the mRNA expression and the catalytic activity of Neu3-overexpressing cells (NEU3) were assessed and compared with the scramble cells (SCR). The results showed an increase in both the

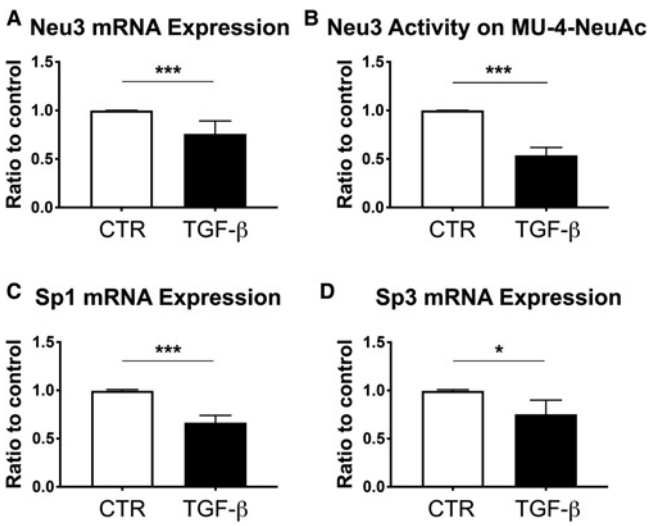

Figure 2. Neu3 expression and activity in cardiac fibroblasts after fibrosis induction.

Fibrosis was induced in cardiac fibroblasts with TGF-β and both the expression and enzymatic activity of sialidase Neu3 were evaluated. (**A**) mRNA expression of Neu3 through RT-PCR. (**B**) Sialidase activity toward 4-MU-NeuAc. (**C**) mRNA expression of Sp1 through RT-PCR. (**D**) ~~Sp3~~ mRNA expression of Sp3 through RT-PCR. Data are presented as mean ± SD of four independent experiments. Results are expressed as fold change, in comparison with untreated cells. Statistical significance was determined by Student's *t*-test. (*)$P < 0.05$; (***)$P < 0.001$.

mRNA expression (300-fold) and enzymatic activity (5-fold) (Supplementary Figure S2A,B). Notably, the overexpression of Neu3 caused the significant decrease in the GM3 levels (2-fold), as expected (Supplementary Figure S2C). These results confirmed the effective overexpression of the active form of Neu3. SCR and NEU3

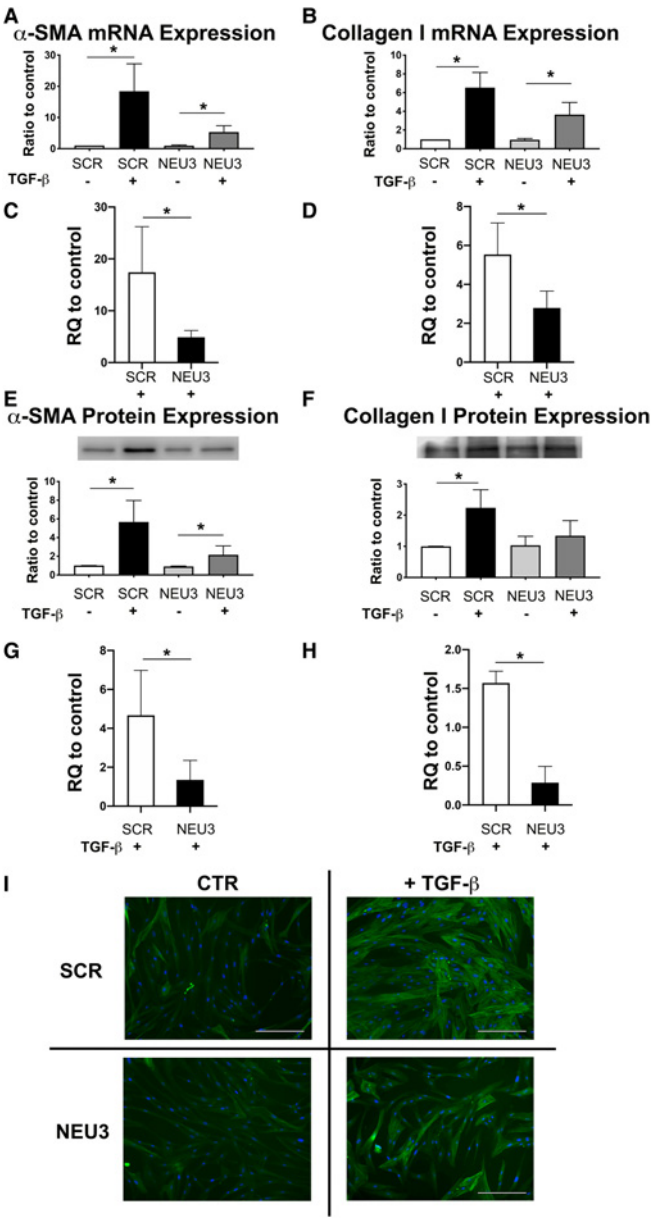

Figure 3. Fibrosis induction in Neu3 overexpressing cells after TGF-β treatment.

Neu3 non-overexpressing (SCR) and Neu3-overexpressing (NEU3) cardiac fibroblasts were treated with TGF-β (10 ng/ml) to induce fibrosis, and the expression of fibrotic markers was analyzed. (**A** and **B**) mRNA expression of α-SMA and collagen I through RT-PCR, as compared with SCR cells. (**C** and **D**) Relative quantity alteration of α-SMA and collagen I mRNA expression in SCR and NEU3 treated-cells, as compared with each correspondent untreated control (**E** and **F**). Protein expression of α-SMA and collagen I through Western Blot analysis. (**G** and **H**) Relative quantity alteration of α-SMA and collagen I protein expression in SCR and NEU3 treated-cells, as compared with each correspondent untreated control. (**I**) Immunofluorescence analysis of α-SMA expression (green) in TGF-β stimulated cells. Cell nuclei were stained with DAPI (blue). Data are presented as mean ± SD of three independent experiments. Scale bar 100 μm. Statistical significance was determined by one-way ANOVA ($P < 0.01$), followed by Bonferroni's test for multiple comparison. (*) $P < 0.05$.

Biochemical Journal (2020) **0** 1–15
https://doi.org/10.1042/BCJ20200360

cells were then treated with TGF-β to induce myofibroblasts differentiation, and the expression of fibrosis markers was evaluated. α-SMA and collagen I showed a significant increase in mRNA expression in both cell lines (Figure 3A,B); however, the increase in both genes in NEU3 treated cells was significantly lower than in SCR cells (Figure 3C,D). Similar results were obtained in the analysis of protein expression, where a significant increase in α-SMA was observed in both cell lines upon TGF-β treatment (Figure 3E), while collagen I was significantly increased only in SCR cells (Figure 3F). In addition, the proteins increase in NEU3 treated cells was significantly lower than in SCR cells (Figure 3G,H). These results were also confirmed morphologically by immunofluorescence analysis of α-SMA: there was a high increase in α-SMA staining in SCR cells after fibroblasts activation, compared with NEU3 cells, in which, conversely, the increase in α-SMA was lower (Figure 3I). Moreover, analysis of the collagen deposition in the extracellular matrix by Sirius Red staining (Figure 4A) was significantly increase after TGF-β treatment in both cell lines (Figure 4B), but the increase was lower in NEU3 cells, compared with SCR cells (Figure 4C).

Neu3 overexpression down-regulated TGF-β pathway activation

The TGF-β pathway is the main pathway implicated in fibrosis onset and progression [18] and GM3 promotes fibrosis through the stabilization of TGF-β R1 [25]. Thus, the activation of the TGF-β pathway after fibrosis induction was evaluated in NEU3 and SCR cells. Results showed an increase in the ratio between phospho-TGF-β R1 and total TGF-β R1 (Figure 5A) and between phospho-SMAD2 and total SMAD2 (Figure 5C) only in SCR cells. This increase was significantly higher, as compared with NEU3 cells (Figure 5B, D). These results indicate an activation of the TGF-β pathway only in SCR cells and not in NEU3 cells. In addition, NEU3 cells showed a significant increase in SMAD7 protein expression, a well-known inhibitor of the TGF-β pathway (Figure 5E,F).

GM3 synthase silencing reduced fibrosis induction

To test whether the observed effects were due to NEU3-induced GM3 depletion and the consequent block of TGF-β pathway activation, we tested whether we could mimic NEU3 overexpression effects by silencing the GM3 synthase to reduce GM3 cell content. To this purpose, cardiac fibroblasts were transfected with specific siRNA duplexes targeting GM3 synthase. Analysis of the GM3 synthase mRNA and protein expression showed a reduction in 70% and 40%, respectively (Supplementary Figure S3A,B); moreover, also the total content of GM3 ganglioside resulted decreased of 30% in shGM3 cells (Supplementary Figure S3C). Then, cells were

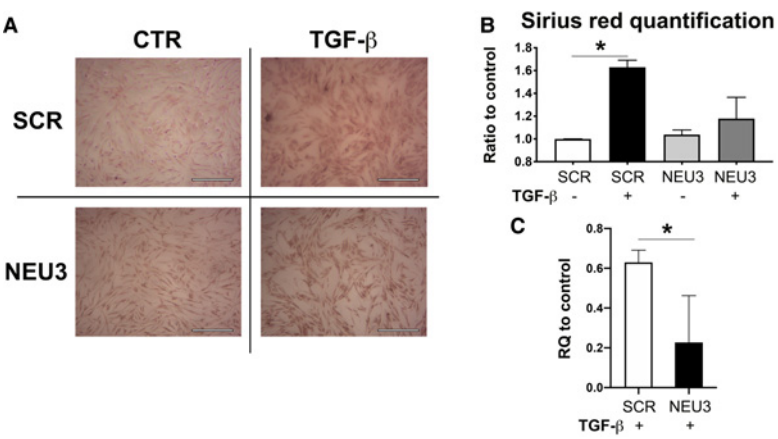

Figure 4. Extracellular protein deposition after fibrosis induction.

(**A**) The deposition of collagen in the extracellular matrix was measured with Sirius Red staining after TGF-β treatment in SCR and NEU3 cardiac fibroblasts. After the staining, the dye was eluted, and the absorbance was measured with a microplate reader. (**B**) Analysis of collagen deposition upon TGF-β treatment, as compared with SCR cells. (**C**) Relative quantity alteration of collagen deposition in SCR and NEU3 treated cells, as compared with each correspondent untreated control. Data are presented as mean ± SD of three independent experiments. Statistical significance was determined by one-way ANOVA ($P < 0.05$), followed by Bonferroni's test for multiple comparison. Scale bar 100 μm. (*) $P < 0.05$.

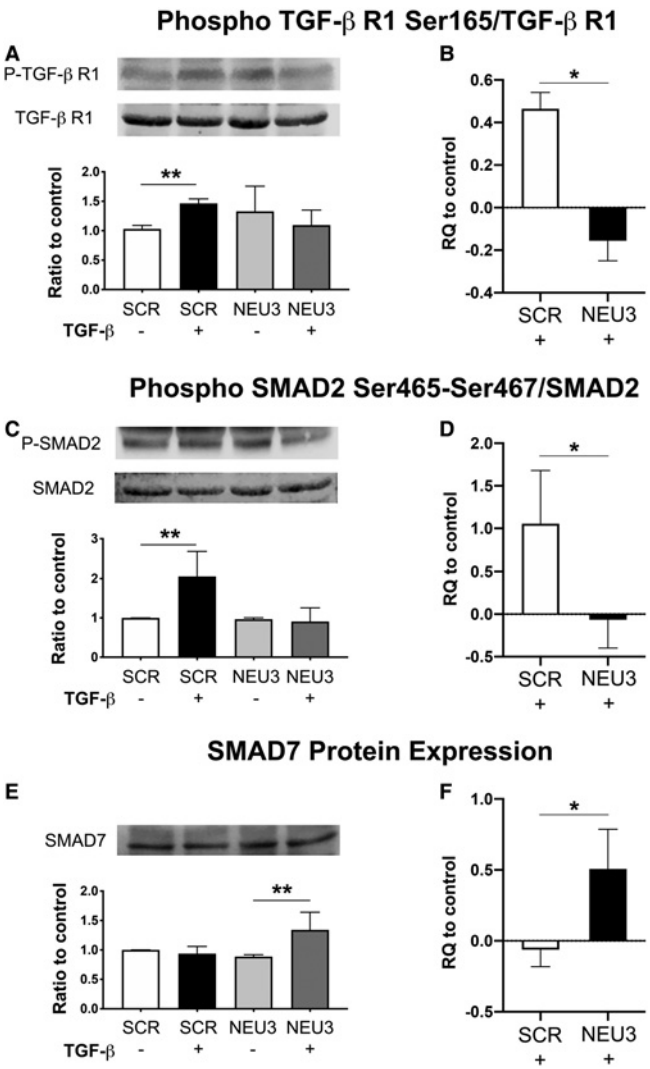

Figure 5. Analysis of TGF-β pathway activation after fibrosis induction.

The activation of the TGF-β pathway was evaluated with Western Blot in SCR and NEU3 cardiac fibroblasts after TGF-β treatment. (**A**) Ratio between phospho-TGF-β Receptor I Ser-165 and total TGF-β Receptor I, as compared with SCR cells. (**B**) Relative quantity alteration of the phospho-TGF-β Receptor I/TGF-β Receptor I ratio in in SCR and NEU3 treated cells, as compared with each correspondent untreated control. (**C**) Ratio between phospho-SMAD2 Ser465/Ser467 and total SMAD2, as compared with SCR cells. (**D**) Relative quantity alteration of the phospho-SMAD2/SMAD2 ratio in in SCR and NEU3 treated cells, as compared with each correspondent untreated control. (**E**) Expression of total SMAD7, as compared with SCR cells. (**F**) Relative quantity alteration of the SMAD7 expression in in SCR and NEU3 treated cells, as compared with each correspondent untreated control. Data are presented as mean ± SD of three independent experiments. Statistical significance was determined by one-way ANOVA ($P < 0.01$), followed by Bonferroni's test for multiple comparison. (*) $P < 0.05$, (**) $P < 0.01$.

treated with TGF-β to induce fibroblasts activation. The results of the mRNA and protein expression of the fibrosis markers were similar to those obtained in the NEU3 cells: in particular, α-SMA and collagen I were increased in both SCR and shGM3 cell lines (Figure 6A,B), even if the increase was significantly lower in shGM3 cells (Figure 6C,D). The same results were also obtained in protein expression of α-SMA and collagen I: a significant protein increase was observed in SCR cells (Figure 6E,F), and the increase in shGM3 cells was significantly lower compared with SCR cells (Figure 6G,H). Moreover, immunofluorescence analysis of α-SMA expression showed a strong increase only in SCR cells (Figure 6E), and also the quantification of ECM proteins

Biochemical Journal (2020) **0** 1–15
https://doi.org/10.1042/BCJ20200360

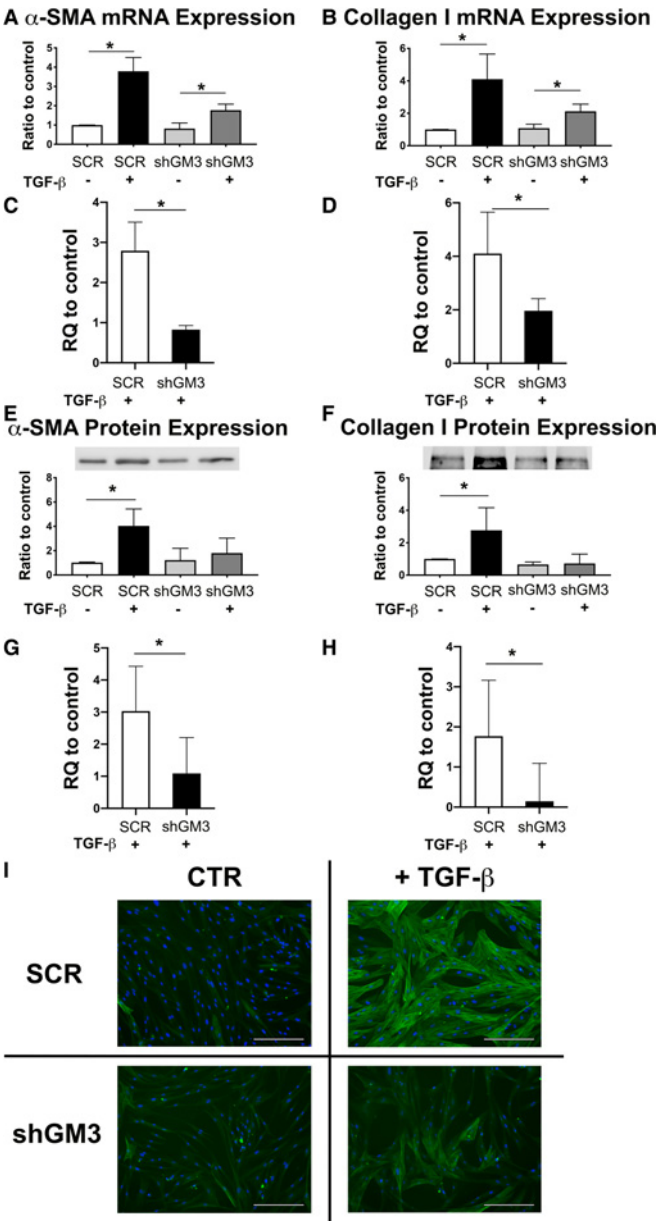

Figure 6. Fibrosis induction in GM3 synthase silenced cells after TGF-β treatment.

Control (SCR) and GM3 synthase silenced (shGM3) cardiac fibroblasts were treated with TGF-β (10 ng/ml) to induce fibrosis, and the expression of fibrotic markers was analyzed. (**A** and **B**) mRNA expression of α-SMA and collagen I through RT-PCR. (**C**,**D**) Relative quantity alteration of α-SMA and collagen I mRNA expression in SCR and shGM3 treated-cells, as compared with each correspondent untreated control (**E** and **F**). Protein expression of α-SMA and collagen I through Western Blot analysis. (**G** and **H**) Relative quantity alteration of α-SMA and collagen I protein expression in SCR and shGM3 treated-cells, as compared with each correspondent untreated control. (**I**) Immunofluorescence analysis of α-SMA expression (green) in TGF-β stimulated cells. Cell nuclei were stained with DAPI (blue). Data are presented as mean ± SD of three independent experiments. Scale bar 100 μm. Statistical significance was determined by one-way ANOVA ($P < 0.01$), followed by Bonferroni's test for multiple comparison. (*) $P < 0.05$.

deposition with Sirius Red staining (Figure 7A) revealed a significant increase in SCR treated-cells (Figure 7B); the increment was significantly higher, as compared with shGM3 cells (Figure 7C), thus confirming the previously observed results.

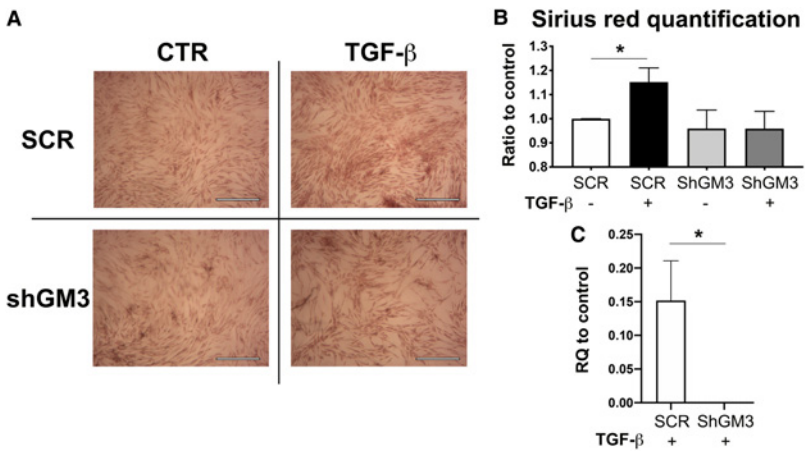

Figure 7. Extracellular protein deposition after fibrosis induction.

(**A**) The deposition of collagen in the extracellular matrix was measured with Sirius Red staining after TGF-β treatment in SCR and shGM3 cardiac fibroblasts. After the staining, the dye was eluted, and the absorbance was measured with a microplate reader. (**B**) Analysis of collagen deposition upon TGF-β treatment, as compared with SCR cells. (**C**) Relative quantity alteration of collagen deposition in SCR and shGM3 treated cells, as compared with each correspondent untreated control. Data are presented as mean ± SD of three independent experiments. Scale bar 100 μm. Statistical significance was determined by one-way ANOVA ($P < 0.01$), followed by Bonferroni's test for multiple comparison. (*) $P < 0.05$.

GM3 synthase silencing inhibited TGF-β pathway

To test whether GM3 synthase silencing had any effect on fibrosis induction, the activation of the pathway was analyzed. As expected, upon TGF-β treatment, activation of the pathway was observed in SCR cells, as confirmed by the significant increase in both the phospho-TGF-β R1/TGF-β R1 (Figure 8A) and phospho-SMAD2/SMAD2 (Figure 8C) ratio. On the other hand, upon fibrosis induction, in shGM3 cells these ratios remained similar to those of untreated cells. Thus, the relative increase in both the phospho-TGF-β R1/TGF-β R1 and phosphor-SMAD2/SMAD2 ratio was significantly higher in SCR cells, as compared with NEU3 cells (Figure 8B,D). Moreover, the expression of the TGF-β receptor type-1 (TGFBR1) inhibitor SMAD7 was significantly increased in shGM3 (Figure 8E), and this increase was significantly higher, as compared with SCR (Figure 8F).

Discussion

In this work, we report that sialidase Neu3 expression and activity are down-regulated during TGF-β-induced cardiac fibrosis. Interestingly, we found a decrease in the two main transcription factors responsible for Neu3 transcription regulation, Sp1 and Sp3 [35], after TGF-β treatment that could explain the mechanism underlying Neu3 decrease. The Neu3 reduction supported the hypothesis that an induced activation of the Neu3 could counteract this degenerative process. Indeed, overexpression of the enzyme significantly decreases the effects of TGF-β on cardiac fibroblasts, reducing their activation toward the myofibroblasts phenotype, as Neu3-overexpressing cells expressed lower levels of α-SMA and they deposited less collagen in the ECM. Encouraged by these results, we investigated the mechanism of Neu3 activity. Indeed, the TGF-β pathway is known to be the principal regulator of fibrosis, and the activation of the signaling cascade is determined by the phosphorylation of TGF-β R1 and R-Smads, with Smad2 playing a central role in the process. Interestingly, Neu3 overexpressing cells, when exposed to TGF-β, exhibited lower levels of both phosphorylated TGF-β R1 and Smad2, indicating a reduced activation of the pathway. In addition, in NEU3 cells, higher levels of Smad7, one of the inhibitory members of the Smad family that acts as a negative feedback inhibitor of the TGF-β pathway, competing with R-Smads for binding with TGF-β R1 could be observed [42]. Overall, these data support that Neu3 overexpression was able to reduce TGF-β pathway activation. In this context, it is known that ganglioside GM3 participates in TGF-β signaling through a direct interaction with TGF-β R1. In fact, GM3 regulates serine phosphorylation of TGF-β R1, TGF-β R2, and Smad2/3, and it is essential for the epithelial-to-mesenchymal transition in human lens epithelial cells [25]. Thus, we envisioned that NEU3 effects

Biochemical Journal (2020) **0** 1–15
https://doi.org/10.1042/BCJ20200360

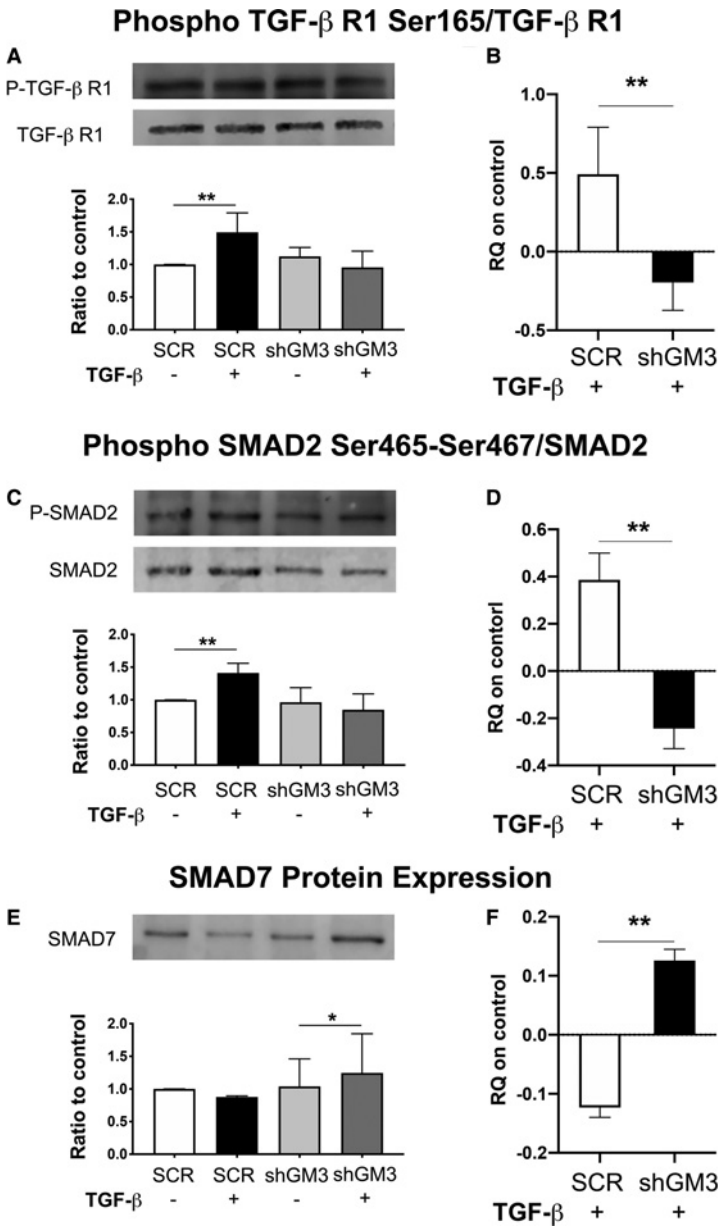

Figure 8. Analysis of TGF-β pathway activation after fibrosis induction.

The activation of the TGF-β pathway was evaluated with Western Blot in SCR and shGM3 cardiac fibroblasts after TGF-β treatment. (**A**) Ratio between phospho-TGF-β Receptor I Ser-165 and total TGF-β Receptor I, as compared with SCR cells. (**B**) Relative quantity alteration of the phospho-TGF-β Receptor I/TGF-β Receptor I ratio in in SCR and shGM3 treated cells, as compared with each correspondent untreated control. (**C**) Ratio between phospho-SMAD2 Ser465/Ser467 and total SMAD2, as compared with SCR cells. (**D**) Relative quantity alteration of the phospho-SMAD2/SMAD2 ratio in in SCR and shGM3 treated cells, as compared with each correspondent untreated control. (**E**) Expression of total SMAD7, as compared with SCR cells. (**F**) Relative quantity alteration of the SMAD7 expression in in SCR and shGM3 treated cells, as compared with each correspondent untreated control. Data are presented as mean ± SD of three independent experiments. Statistical significance was determined by one-way ANOVA ($P < 0.01$), followed by Bonferroni's test for multiple comparison. (*) $P < 0.05$, (**) $P < 0.01$.

could be mediated by the enzyme's ability to regulate GM3 levels. Along with this line, we previously demonstrated the pivotal role of Neu3 in regulating the intracellular levels of GM3 [31,34,35], also in ~~NEU3~~ cardiac fibroblasts [36], even by the enzyme trans-activity on the gangliosides of adjacent cells [33]. To test our

hypothesis, we mimicked the effect of Neu3 overexpression by silencing GM3 synthase. Remarkably, the reduction in both the mRNA and protein expression of GM3 synthase caused similar effects on fibrosis inhibition as we observed for Neu3 overexpression. Thus, these results support the notion that Neu3 effects could be mediated by a reduction in cellular GM3 levels that, in turn, could reduce the stabilization and activity of TGF-β R1. Indeed, the involvement of sialidase Neu3 in the fibrotic process has also been described in the lungs. However, Chen and coworkers [43] observed a decrease in Neu3 degradation, accompanied by an increase in its translation within lung epithelial cells, suggesting that Neu3 could behave as an inducer of pulmonary fibrosis. While these results seem to be in contrast with our data, it has been demonstrated that the response to TGF-β is organ- [44] and even cell-specific [45]. In fact, it is known that cardiac and pulmonary fibrosis significantly differ in their etiology [46]. In particular, the major source of the pulmonary mediators for fibroblasts activation and differentiation are the lung epithelial cells [46], whereas, in the myocardium, the onset is given by inflammation, which, in turn, triggers the fibroblasts-myofibroblast conversion [47]. Indeed, based on previous reports, the molecular response to TGF-β treatment is likely to be different in cardiac fibroblasts and epithelial cells [45]. Nonetheless, in our work, we found that Neu3 overexpression or GM3 synthase silencing could completely block TGF-β-induced fibroblasts activation. This apparent limitation could turn out being of critical importance from a translational perspective. In fact, after tissue injury, an initial fibrotic response has been shown to be critical for avoiding cardiac wall rupture, eventually maintaining organ integrity. On the other hand, an uncontrolled fibrosis progression leads to a deep remodeling of the heart, including chamber dilatation, cardiomyocytes hypertrophy, an increased risk of arrhythmogenesis, and the development of congestive heart failure [48]. Thus, the ideal antifibrotic therapy should be able to fine-tune fibrosis progression, and it is usually started after an unexpected initial acute event. To date, no efficient antifibrotic therapies are available to the clinic, and heart transplantation cannot be considered a therapeutic option for the general population. While new regenerative strategies are emerging [49,50], the identification of Neu3 and GM3 as possible new targets for pharmacological treatment is of great value. To this end, this work supports that sialidase NEU3 and GM3 are new players in cardiac fibrosis, and the modulation of their content should be further assessed for a possible therapeutic application.

Competing Interests

Q2 The authors declare that there are no competing interests associated with the manuscript.

Q3 **Funding**

This study was partially supported by Ricerca Corrente funding from Italian Ministry of Health to IRCCS Policlinico San Donato.

Author Contributions

Conceptualization: A.G., M.P., L.A.; Methodology: A.G., M.P., F.C.; Formal analysis and investigation: A.G., M.P., P.C., S.D'I., P.R., A.G., M.A., E.V.C.; Writing — original draft preparation: A.G., M.P.; Writing— review and editing: A.G., M.P., E.M., M.M.M., G.C., L.M., C.P., L.A.; Funding acquisition: L.A.; Supervision: L.A., C.P.

Abbreviations

DAPI, diamino-2-phenylindole; ECM, extracellular matrix; ECM, extracellular matrix; FBS, fetal bovine serum; PBS, phosphate buffer solution; SCR, scramble cells; TGF-β, transforming growth factor beta; α-SMA, anti-α-Smooth muscle actin; α-SMA, α-smooth muscle actin.

References

1 Sun, Y.B., Qu, X., Caruana, G. and Li, J. (2016) The origin of renal fibroblasts/myofibroblasts and the signals that trigger fibrosis. *Differentiation* **92**, 102–107 https://doi.org/10.1016/j.diff.2016.05.008

2 Campana, L. and Iredale, J.P. (2017) Regression of liver fibrosis. *Semin. Liver Dis.* **37**, 1–10 https://doi.org/10.1055/s-0036-1597816

3 Gulati, S. and Thannickal, V.J. (2019) The aging lung and idiopathic pulmonary fibrosis. *Am. J. Med. Sci.* **357**, 384–389 https://doi.org/10.1016/j.amjms.2019.02.008

4 Travers, J.G., Kamal, F.A., Robbins, J., Yutzey, K.E. and Blaxall, B.C. (2016) Cardiac fibrosis: the fibroblast awakens. *Circ. Res.* **118**, 1021–1040 https://doi.org/10.1161/CIRCRESAHA.115.306565

5 Ma, Z.G., Yuan, Y.P., Wu, H.M., Zhang, X. and Tang, Q.Z. (2018) Cardiac fibrosis: new insights into the pathogenesis. *Int. J. Biol. Sci.* **14**, 1645–1657 https://doi.org/10.7150/ijbs.28103

6 Frangogiannis, N.G. (2019) Cardiac fibrosis: Cell biological mechanisms, molecular pathways and therapeutic opportunities. *Mol. Aspects Med.* **65**, 70–99 https://doi.org/10.1016/j.mam.2018.07.001
7 Jiang, S., Li, T., Yang, Z., Yi, W., Di, S., Sun, Y. et al. (2017) AMPK orchestrates an elaborate cascade protecting tissue from fibrosis and aging. *Ageing Res. Rev.* **38**, 18–27 https://doi.org/10.1016/j.arr.2017.07.001
8 Rockey, D.C., Bell, P.D. and Hill, J.A. (2015) Fibrosis–a common pathway to organ injury and failure. *N. Engl. J. Med.* **372**, 1138–1149 https://doi.org/10.1056/NEJMra1300575
9 Bergmann, O., Bhardwaj, R.D., Bernard, S., Zdunek, S., Barnabe-Heider, F., Walsh, S. et al. (2009) Evidence for cardiomyocyte renewal in humans. *Science* **324**, 98–102 https://doi.org/10.1126/science.1164680
10 Park, S., Nguyen, N.B., Pezhouman, A. and Ardehali, R. (2019) Cardiac fibrosis: potential therapeutic targets. *Transl. Res.* **209**, 121–137 https://doi.org/10.1016/j.trsl.2019.03.001
11 Fan, D., Takawale, A., Lee, J. and Kassiri, Z. (2012) Cardiac fibroblasts, fibrosis and extracellular matrix remodeling in heart disease. *Fibrogenesis Tissue Repair* **5**, 15 https://doi.org/10.1186/1755-1536-5-15
12 Moore-Morris, T., Guimaraes-Camboa, N., Banerjee, I., Zambon, A.C., Kisseleva, T., Velayoudon, A. et al. (2014) Resident fibroblast lineages mediate pressure overload-induced cardiac fibrosis. *J. Clin. Invest.* **124**, 2921–2934 https://doi.org/10.1172/JCI74783
13 Hortells, L., Johansen, A.K.Z. and Yutzey, K.E. (2019) Cardiac fibroblasts and the extracellular matrix in regenerative and nonregenerative hearts. *J. Cardiovasc. Dev. Dis.* **6**, 29 https://doi.org/10.3390/jcdd6030029
14 Vasquez, C., Benamer, N. and Morley, G.E. (2011) The cardiac fibroblast: functional and electrophysiological considerations in healthy and diseased hearts. *J. Cardiovasc. Pharmacol.* **57**, 380–388 https://doi.org/10.1097/FJC.0b013e31820cda19
15 Frangogiannis, N.G. (2014) The inflammatory response in myocardial injury, repair, and remodelling. *Nat. Rev. Cardiol.* **11**, 255–265 https://doi.org/10.1038/nrcardio.2014.28
16 Prunotto, M., Bruschi, M., Gunning, P., Gabbiani, G., Weibel, F., Ghiggeri, G.M. et al. (2015) Stable incorporation of alpha-smooth muscle actin into stress fibers is dependent on specific tropomyosin isoforms. *Cytoskeleton (Hoboken)* **72**, 257–267 https://doi.org/10.1002/cm.21230
17 Meng, X.M., Nikolic-Paterson, D.J. and Lan, H.Y. (2016) TGF-beta: the master regulator of fibrosis. *Nat. Rev. Nephrol.* **12**, 325–338 https://doi.org/10.1038/nrneph.2016.48
18 Khalil, H., Kanisicak, O., Prasad, V., Correll, R.N., Fu, X., Schips, T. et al. (2017) Fibroblast-specific TGF-beta-Smad2/3 signaling underlies cardiac fibrosis. *J. Clin. Invest.* **127**, 3770–3783 https://doi.org/10.1172/JCI94753
19 Huang, F. and Chen, Y.G. (2012) Regulation of TGF-beta receptor activity. *Cell Biosci.* **2**, 9 https://doi.org/10.1186/2045-3701-2-9
20 Imamura, T., Oshima, Y. and Hikita, A. (2013) Regulation of TGF-beta family signalling by ubiquitination and deubiquitination. *J. Biochem.* **154**, 481–489 https://doi.org/10.1093/jb/mvt097
21 Ray, B.N., Lee, N.Y., How, T. and Blobe, G.C. (2010) ALK5 phosphorylation of the endoglin cytoplasmic domain regulates Smad1/5/8 signaling and endothelial cell migration. *Carcinogenesis* **31**, 435–441 https://doi.org/10.1093/carcin/bgp327
22 Nickel, J., Ten Dijke, P. and Mueller, T.D. (2018) TGF-beta family co-receptor function and signaling. *Acta Biochim. Biophys. Sin. (Shanghai)* **50**, 12–36 https://doi.org/10.1093/abbs/gmx126
23 Yakymovych, I., Yakymovych, M. and Heldin, C.H. (2018) Intracellular trafficking of transforming growth factor beta receptors. *Acta Biochim. Biophys. Sin. (Shanghai)* **50**, 3–11 https://doi.org/10.1093/abbs/gmx119
24 Moreno-Caceres, J., Caja, L., Mainez, J., Mayoral, R., Martin-Sanz, P., Moreno-Vicente, R. et al. (2014) Caveolin-1 is required for TGF-beta-induced transactivation of the EGF receptor pathway in hepatocytes through the activation of the metalloprotease TACE/ADAM17. *Cell Death Dis.* **5**, e1326 https://doi.org/10.1038/cddis.2014.294
25 Kim, S.J., Chung, T.W., Choi, H.J., Kwak, C.H., Song, K.H., Suh, S.J. et al. (2013) Ganglioside GM3 participates in the TGF-beta1-induced epithelial-mesenchymal transition of human lens epithelial cells. *Biochem. J.* **449**, 241–251 https://doi.org/10.1042/BJ20120189
26 Bergante, S., Creo, P., Piccoli, M., Ghiroldi, A., Menon, A., Cirillo, F. et al. (2018) GM1 ganglioside promotes osteogenic differentiation of human tendon stem cells. *Stem Cells Int.* **2018**, 4706943 https://doi.org/10.1155/2018/4706943
27 Bergante, S., Torretta, E., Creo, P., Sessarego, N., Papini, N., Piccoli, M. et al. (2014) Gangliosides as a potential new class of stem cell markers: the case of GD1a in human bone marrow mesenchymal stem cells. *J. Lipid Res.* **55**, 549–560 https://doi.org/10.1194/jlr.M046672
28 Russo, D., Parashuraman, S. and D'Angelo, G. (2016) Glycosphingolipid-protein interaction in signal transduction. *Int. J. Mol. Sci* **17**, 1732 https://doi.org/10.3390/ijms17101732
29 Inokuchi, J.I., Inamori, K.I., Kabayama, K., Nagafuku, M., Uemura, S., Go, S. et al. (2018) Biology of GM3 ganglioside. *Prog. Mol. Biol. Transl. Sci.* **156**, 151–195 https://doi.org/10.1016/bs.pmbts.2017.10.004
30 Gu, X.B., Gu, T.J. and Yu, R.K. (1990) Purification to homogeneity of GD3 synthase and partial purification of GM3 synthase from rat brain. *Biochem. Biophys. Res. Commun.* **166**, 387–393 https://doi.org/10.1016/0006-291X(90)91957-T
31 Anastasia, L., Papini, N., Colazzo, F., Palazzolo, G., Tringali, C., Dileo, L. et al. (2008) NEU3 sialidase strictly modulates GM3 levels in skeletal myoblasts C2C12 thus favoring their differentiation and protecting them from apoptosis. *J. Biol. Chem.* **283**, 36265–36271 https://doi.org/10.1074/jbc.M805755200
32 Tringali, C., Lupo, B., Cirillo, F., Papini, N., Anastasia, L., Lamorte, G. et al. (2009) Silencing of membrane-associated sialidase Neu3 diminishes apoptosis resistance and triggers megakaryocytic differentiation of chronic myeloid leukemic cells K562 through the increase of ganglioside GM3. *Cell Death Differ.* **16**, 164–174 https://doi.org/10.1038/cdd.2008.141
33 Papini, N., Anastasia, L., Tringali, C., Croci, G., Bresciani, R., Yamaguchi, K. et al. (2004) The plasma membrane-associated sialidase MmNEU3 modifies the ganglioside pattern of adjacent cells supporting its involvement in cell-to-cell interactions. *J. Biol. Chem.* **279**, 16989–16995 https://doi.org/10.1074/jbc.M400881200
34 Papini, N., Anastasia, L., Tringali, C., Dileo, L., Carubelli, I., Sampaolesi, M. et al. (2012) MmNEU3 sialidase over-expression in C2C12 myoblasts delays differentiation and induces hypertrophic myotube formation. *J. Cell Biochem.* **113**, 2967–2978 https://doi.org/10.1002/jcb.24174
35 Scaringi, R., Piccoli, M., Papini, N., Cirillo, F., Conforti, E., Bergante, S. et al. (2013) NEU3 sialidase is activated under hypoxia and protects skeletal muscle cells from apoptosis through the activation of the epidermal growth factor receptor signaling pathway and the hypoxia-inducible factor (HIF)-1alpha. *J. Biol. Chem.* **288**, 3153–3162 https://doi.org/10.1074/jbc.M112.404327

36 Piccoli, M., Conforti, E., Varrica, A., Ghiroldi, A., Cirillo, F., Resmini, G. et al. (2017) NEU3 sialidase role in activating HIF-1alpha in response to chronic hypoxia in cyanotic congenital heart patients. *Int. J. Cardiol.* **230**, 6–13 https://doi.org/10.1016/j.ijcard.2016.12.123
37 Cirillo, F., Ghiroldi, A., Fania, C., Piccoli, M., Torretta, E., Tettamanti, G. et al. (2016) NEU3 sialidase protein interactors in the plasma membrane and in the endosomes. *J. Biol. Chem.* **291**, 10615–10624 https://doi.org/10.1074/jbc.M116.719518
38 Rota, P., Cirillo, F., Piccoli, M., Gregorio, A., Tettamanti, G., Allevi, P. et al. (2015) Synthesis and biological evaluation of several dephosphonated analogues of CMP-Neu5Ac as inhibitors of GM3-synthase. *Chemistry* **21**, 14614–14629 https://doi.org/10.1002/chem.201501770
39 Tullberg-Reinert, H. and Jundt, G. (1999) In situ measurement of collagen synthesis by human bone cells with a sirius red-based colorimetric microassay: effects of transforming growth factor beta2 and ascorbic acid 2-phosphate. *Histochem. Cell Biol.* **112**, 271–276 https://doi.org/10.1007/s004180050447
40 Halfon, S., Abramov, N., Grinblat, B. and Ginis, I. (2011) Markers distinguishing mesenchymal stem cells from fibroblasts are downregulated with passaging. *Stem Cells Dev.* **20**, 53–66 https://doi.org/10.1089/scd.2010.0040
41 Denu, R.A., Nemcek, S., Bloom, D.D., Goodrich, A.D., Kim, J., Mosher, D.F. et al. (2016) Fibroblasts and mesenchymal stromal/stem cells are phenotypically indistinguishable. *Acta Haematol.* **136**, 85–97 https://doi.org/10.1159/000445096
42 Yan, X. and Chen, Y.G. (2011) Smad7: not only a regulator, but also a cross-talk mediator of TGF-beta signalling. *Biochem. J.* **434**, 1–10 https://doi.org/10.1042/BJ20101827
43 Chen, W., Lamb, T.M. and Gomer, R.H. (2020) TGF-beta1 increases sialidase 3 expression in human lung epithelial cells by decreasing its degradation and upregulating its translation. *Exp. Lung Res.* **46**, 75–80 https://doi.org/10.1080/01902148.2020.1733135
44 Pohlers, D., Brenmoehl, J., Loffler, I., Muller, C.K., Leipner, C., Schultze-Mosgau, S. et al. (2009) TGF-beta and fibrosis in different organs - molecular pathway imprints. *Biochim. Biophys. Acta* **1792**, 746–756 https://doi.org/10.1016/j.bbadis.2009.06.004
45 Guo, X., Hutcheon, A.E.K., Tran, J.A. and Zieske, J.D. (2017) TGF-beta-target genes are differentially regulated in corneal epithelial cells and fibroblasts. *New Front. Ophthalmol.* **3**, 10.15761/NFO.1000151 https://doi.org/10.15761/NFO.1000151
46 Murtha, L.A., Schuliga, M.J., Mabotuwana, N.S., Hardy, S.A., Waters, D.W., Burgess, J.K. et al. (2017) The processes and mechanisms of cardiac and pulmonary fibrosis. *Front. Physiol.* **8**, 777 https://doi.org/10.3389/fphys.2017.00777
47 Van Linthout, S., Miteva, K. and Tschope, C. (2014) Crosstalk between fibroblasts and inflammatory cells. *Cardiovasc. Res.* **102**, 258–269 https://doi.org/10.1093/cvr/cvu062
48 Gonzalez, A., Schelbert, E.B., Diez, J. and Butler, J. (2018) Myocardial interstitial fibrosis in heart failure: biological and translational perspectives. *J. Am. Coll. Cardiol.* **71**, 1696–1706 https://doi.org/10.1016/j.jacc.2018.02.021
49 Ghiroldi, A., Piccoli, M., Ciconte, G., Pappone, C. and Anastasia, L. (2017) Regenerating the human heart: direct reprogramming strategies and their current limitations. *Basic Res. Cardiol.* **112**, 68 https://doi.org/10.1007/s00395-017-0655-9
50 Ghiroldi, A., Piccoli, M., Cirillo, F., Monasky, M.M., Ciconte, G., Pappone, C. et al. (2018) Cell-based therapies for cardiac regeneration: a comprehensive review of past and ongoing strategies. *Int. J. Mol. Sci.* **19**, 3194 https://doi.org/10.3390/ijms19103194